

## Role of ocean in the genesis and annihilation of the core of the warm pool in the southeastern Arabian Sea

S. C. SHENOI, D. SHANKAR, V. V. GOPALAKRISHNA and F. DURAND\*

*National Institute of Oceanography, Dona Paula, Goa - 403 004, India*

e mail: ShenoI @darya.nio.org

सार – आरमेक्स (अरब सागर मानसून प्रयोग) विज्ञान योजना में बताए गए पूर्ववर्ती अनुमान की दक्षिणी पूर्वी अरब सागर में उष्ण जलकुंड के कोर की उत्पत्ति में महासागर की अत्यंत महत्वपूर्ण किंतु निष्क्रिय भूमिका होती है; इसकी जाँच आरमेक्स के दूसरे चरण के दौरान एकत्रित किए गए नए आँकड़ों के परिप्रेक्ष्य में की गई है। इस शोध-पत्र में संक्षेप यह बताया गया है कि इन आँकड़ों के आधार पर प्राप्त हुए परिणामों से यह पता चलता है कि न केवल दक्षिणी पूर्वी अरब सागर में उष्ण जलकुंड की उत्पत्ति के समय में बल्कि उष्ण जलकुंड को कम करने में भी अप्रत्यक्ष रूप से प्रबल महासागरीय गतिकों की सक्रिय, न कि निष्क्रिय, भूमिका रहती है।

ABSTRACT. The earlier hypothesis, stated in the ARMEX (Arabian Sea Monsoon Experiment) Science Plan, that the ocean plays an important, but passive, role in the genesis of the core of warm pool in the southeastern Arabian Sea (SEAS) is examined in the light of new data collected during Phase II of ARMEX. The new evidence confirms that the ocean plays an important role. This paper summarises the results based on these data, which show that the remotely forced ocean dynamics plays an active, not passive, role not only in the genesis of the core of the warm pool in the SEAS, but also triggers the collapse of the warm pool.

**Key words** - ARMEX, North Indian Ocean, Warm Pool, Salinity, Coastal Kelvin wave.

### I. Introduction

The North Indian Ocean (NIO) becomes the warmest amongst the world oceans prior to the onset of summer monsoon (Joseph, 1990). The extent of this region, known as 'Indian Ocean Warm Pool' (IOWP), increases from 14 million km<sup>2</sup> in February to 24 million km<sup>2</sup> in April and then decreases to 8 million km<sup>2</sup> in September (Vinayachandran and Shetye, 1991). In the Arabian Sea, the core of this warm pool lies in the Lakshadweep Sea, the part of the southeastern Arabian Sea (SEAS) between the Indian peninsula and the Lakshadweep islands to the west of the Indian mainland. Rao and Sivakumar (1999) called the warm area in the SEAS a 'mini-warm pool' (MWP). ShenoI *et al.*, (1999) called the core MWP 'Sea surface temperature (SST) High' (SSTH), and showed that it develops in the Lakshadweep Sea in February-March, well before the large-scale warming that occurs in the NIO. They argued that the SSTH is intimately connected to the sea-level high, called Lakshadweep high (LH) (Bruce *et al.*, 1994, 1998; Shankar and Shetye, 1997) that forms in the SEAS during December.

Rao and Sivakumar (1999) also underlined the role played by the ocean in the formation of the MWP in the SEAS. They concluded that the near-surface stratification due to the arrival of low-salinity water from the Bay of Bengal during winter (November-February) is important for the formation of warm pool in the SEAS. Subsequently, in March-April, under clear sky and light-wind conditions, the radiative heat input overwhelms the turbulent heat loss at the air-sea interface and the net surplus heat energy is absorbed in a shallow, low-salinity, stratified near-surface layer, resulting in the formation of the MWP. During March-April, the mixed layer in the IOWP warms quickly, in response to positive net surface flux and penetrative solar radiation (Sengupta *et al.*, 2002).

ShenoI *et al.*, (1999) also highlighted the requirement of low-salinity water in the SEAS for the formation of the SSTH in February-March, well before the general warming that takes place all over the NIO. They argued that the SSTH has its genesis in events that occur about 6 months earlier in the Bay of Bengal, when the

\*Current affiliation : LEGOS-IRD-UMR5566, 14 Av. E. Belin, 31400 Toulouse, France

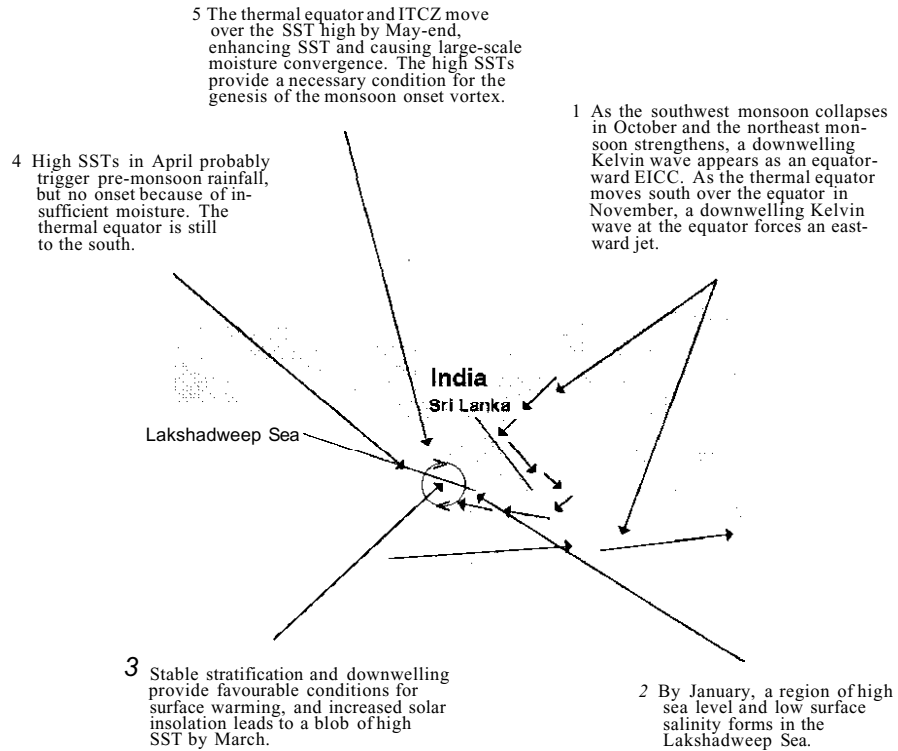
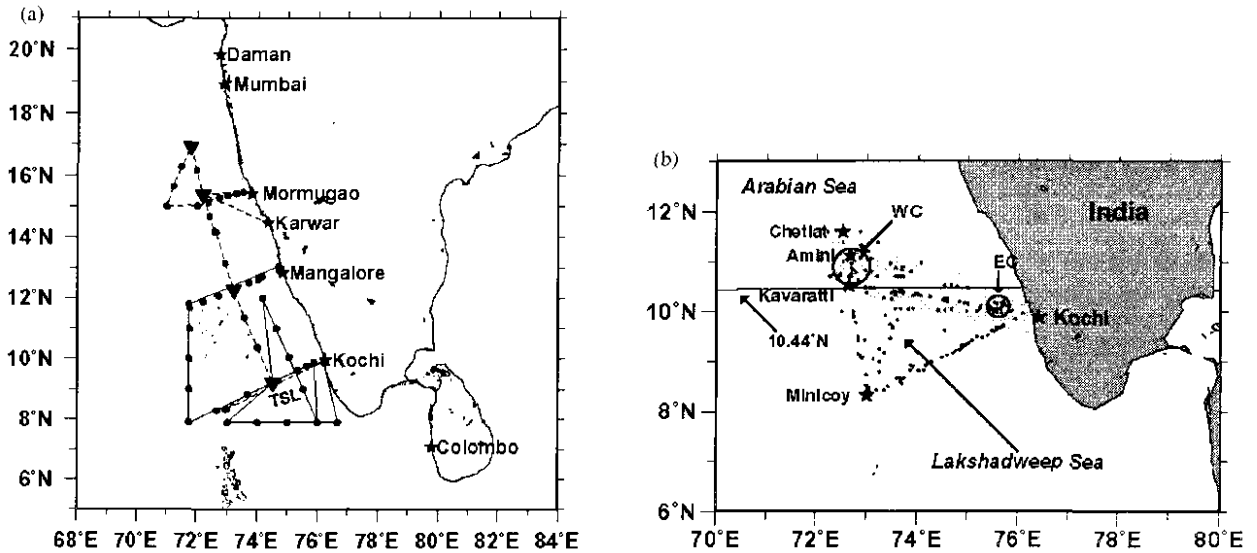


Fig. 1. Schematic summarizing the process that leads to the formation of the pre-monsoon SST high and, perhaps, the monsoon onset vortex. Reproduced from Shenoi *et al.*, (1999)



Figs. 2 (a&b). (a) The tracks of two cruises undertaken on board ORV Sagar Kanya in the SEAS during 14 March - 10 April 2003 (solid line) and 15 May - 19 June 2003 (broken line). TSL indicates the time-series location occupied during both cruises for 2 hourly CTD measurements. The triangles indicate the position of short-duration time-series measurements occupied during June 2003. The black dots along the track indicate the CTD station locations and (b) The region of XBT surveys during May 2002 to April 2004 in the Lakshadweep Sea. The feeder ships for the islands in the Lakshadweep chain were used for the XBT surveys. The black dots mark the location of XBT profiles and surface water samples collected for salinity analysis. The two circles, EC and WC, indicate the location of XBT profiles used for Fig. 12 and the locations of surface salinity used in Fig. 8. The shaded band indicates the location of stations that constitute the best sampled section; data from this section were used for Fig. 12

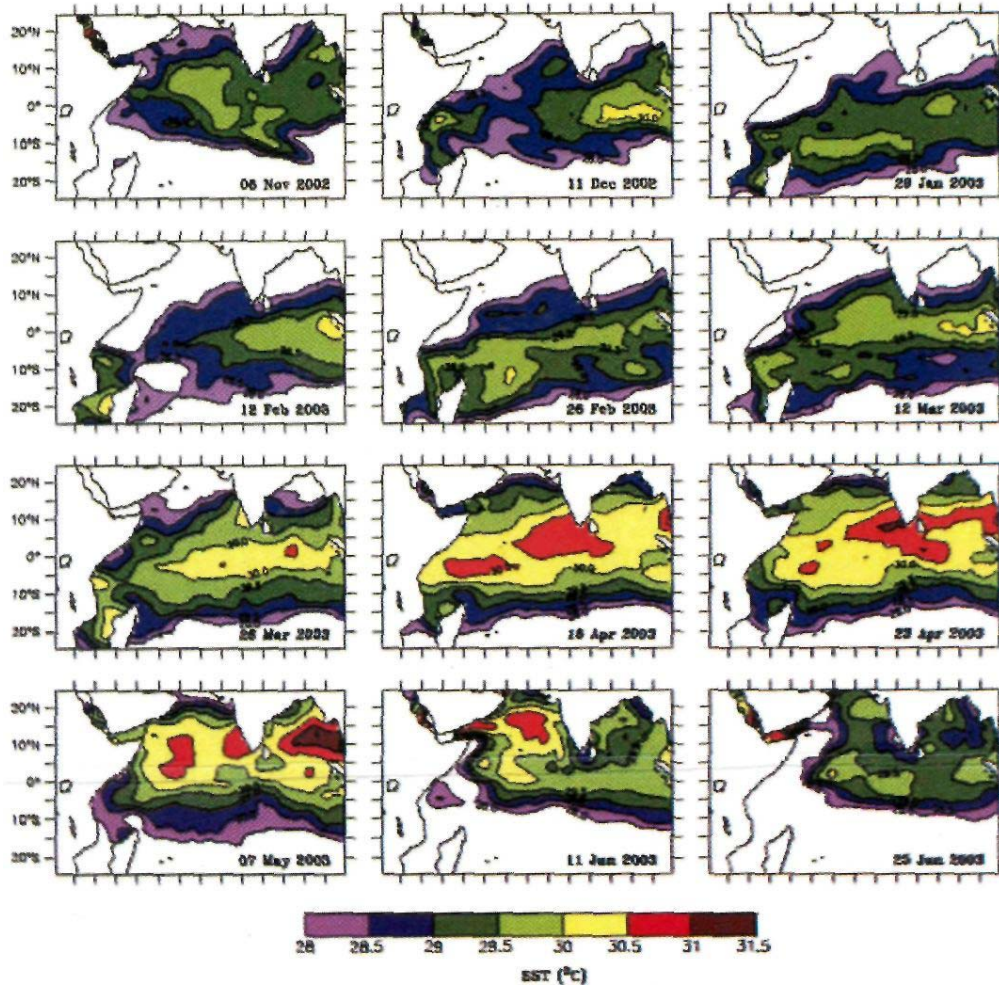


Fig. 3. Evolution of weekly SST ( $^{\circ}\text{C}$ ), based on the data of Reynolds and Smith (1994) in the north Indian Ocean during November 2002 - June 2003. The SST high (SSTH) first appears in the SEAS in early March; it retains its identity even within the warm pool that engulfs the Arabian Sea in May. In May, the SSTH acts as the core of IOWP. Cooling is also seen first in the SEAS late in May, when most of the Arabian Sea is still warm

summer monsoon collapses and the winds reverse direction. The wind reversal generates a down welling coastal Kelvin wave along the periphery of the Bay of Bengal, which ultimately propagates into the SEAS. On its arrival in the SEAS, the down welling Kelvin wave radiates down welling Rossby waves, which propagate westward, leading to the generation of a high in sea level, the LH, in the region (Shankar and Shetye, 1997). The down welling Kelvin wave along the east coast of India also forces an equator ward East India Coastal Current (EICC) (Shankar *et al.*, 1996; McCreary *et al.*, 1996; Vinayachandran *et al.*, 1996; Shankar *et al.*, 2002), which brings low-salinity water from the Bay to the SEAS (Shetye *et al.*, 1996; Shankar, 2000; Han

and McCreary, 2001; Shankar *et al.*, 2002). The LH, together with the low-salinity water, ensures that the ocean does nothing to kill an increase in SST, and the ocean thereby provides the necessary breeding ground for the formation of the SSTH. In February-March, when there is an increase in solar insolation, the SEAS warms faster than the rest of the basin, leading to the formation of the MWP with the SSTH forming its core in the Lakshadweep Sea. Later in May, prior to the onset of summer monsoon, the entire basin warms (Shenoi *et al.*, 2002). Even then, the SSTH retains its identity, maintaining a temperature of about  $0.5^{\circ}\text{C}$  higher than the surroundings, which constitute the IOWP in the Arabian Sea.

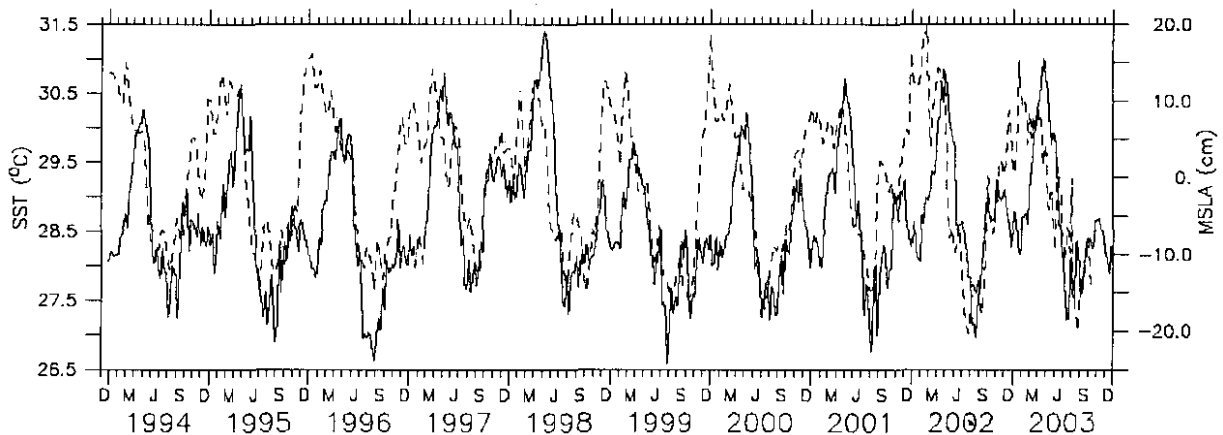


Fig. 4. Interannual variability of SST ( $^{\circ}\text{C}$ ; solid line) and sea level anomaly (SLA, cm; broken line) in the Lakshadweep Sea ( $8\text{--}10^{\circ}\text{N}$ ;  $74\text{--}76^{\circ}\text{E}$ ) during the last decade (1994-2003). The data source for SST is same as in Fig. 3, and SLA data are from the TOPEX/Poseidon altimeter. Note the lag between SST and SLA peaks

The interest in the MWP and SSTH grew due to their possible link with the monsoon 'onset vortex' that often, but not always, heralds the onset of the summer monsoon over the Indian mainland (Shenoi *et al.*, 1999; Rao and Sivakumar, 1999). The monsoon onset vortex has a tendency to form over the SEAS (Krishnamurti *et al.*, 1981). The possibility of a connection between the warm pool and the onset vortex, summarised in the schematic in Fig. 1 (after Shenoi *et al.*, 1999), was the basis for the design of the implementation plan for Phase II of the Arabian Sea Monsoon Experiment (ARMEX-II), ARMEX-II was designed to understand the events that led to the existence of the MWP in the SEAS, particularly the SSTH in the Lakshadweep Sea, and to investigate the possible coupling between the warm SSTs and the process of monsoon onset. Accordingly, two cruises were planned and carried out on board ORV Sagar Kanya to measure the oceanic and atmospheric parameters during the growing and mature phases of the warm pool; the first cruise was during 14 March to 10 April 2003 and the second was during 15 May to 19 June 2003 [Fig. 2(a) for the cruise tracks]. In addition to these observations, twice-monthly Expendable Bathy Thermograph (XBT) surveys were conducted during May 2002 to April 2004 using feeder ships plying between Kochi on the mainland and the Lakshadweep Islands [Fig. 2(b)]. Several moored buoys equipped with sensors for SST, salinity, air temperature, etc. were also available in the vicinity of Lakshadweep Sea. The findings from this experiment, published recently, confirm the crucial role played by the ocean in the formation and decay of the core of warm pool in the SEAS. In this paper, we review these results and concatenate various processes to show that ocean dynamics plays an active role in the life cycle of the warm pool.

## 2. Evolution of SST and sea level in the Arabian Sea during 2002-2003

A series of weekly SST fields during November 2002 to June 2003 is shown in Fig. 3. For the week centered on 6 November 2002 SST is higher than  $28^{\circ}\text{C}$  in the SEAS as well as in a band extending from  $10^{\circ}\text{S}$  to  $10^{\circ}\text{N}$ . In the week centered 11 December 2002, the band of warm SST shrank considerably. SST exceeding  $28^{\circ}\text{C}$  during November-December in the NIO is unusual, and is due to the unusually weak monsoon of 2002 (Gadgil *et al.*, 2002), which left behind a warm NIO. In late January 2003, SST in the SEAS was below  $28^{\circ}\text{C}$ . The band of high SST, seen only in the south (around  $10^{\circ}\text{S}$ ), reflects the position of the Sun, and hence, of the region of maximum solar insolation. The TCZ (Tropical Convergence Zone) roughly corresponds to this band of high SST. Subsequent Figures for January-February show the northward migration of this band associated with the northward movement of the Sun. Later, for the week centered 26 March, a blob of high SST, distinct from the warm SST band associated with the TCZ, forms in the Lakshadweep Sea; this is the SSTH described by Shenoi *et al.*, (1999). With time, the blob grows toward west-southwest, and by mid-April, it extends across the southern Arabian Sea; this is the MWP described by Rao and Sivakumar (1999). Simultaneously, the band of high SST located south also migrates towards north; it extends till  $15^{\circ}\text{N}$  in the week centered 26 March. In mid-April (around 16 April 2003), the zonal band of high SST runs over the SSTH, but even then the SSTH retains its identity within the IOWP, its temperature being about  $0.5^{\circ}\text{C}$  higher than that in the rest of the IOWP. In the week centered 11 June, the SEAS starts cooling, and the SSTH vanishes, giving way to a blob of low SST

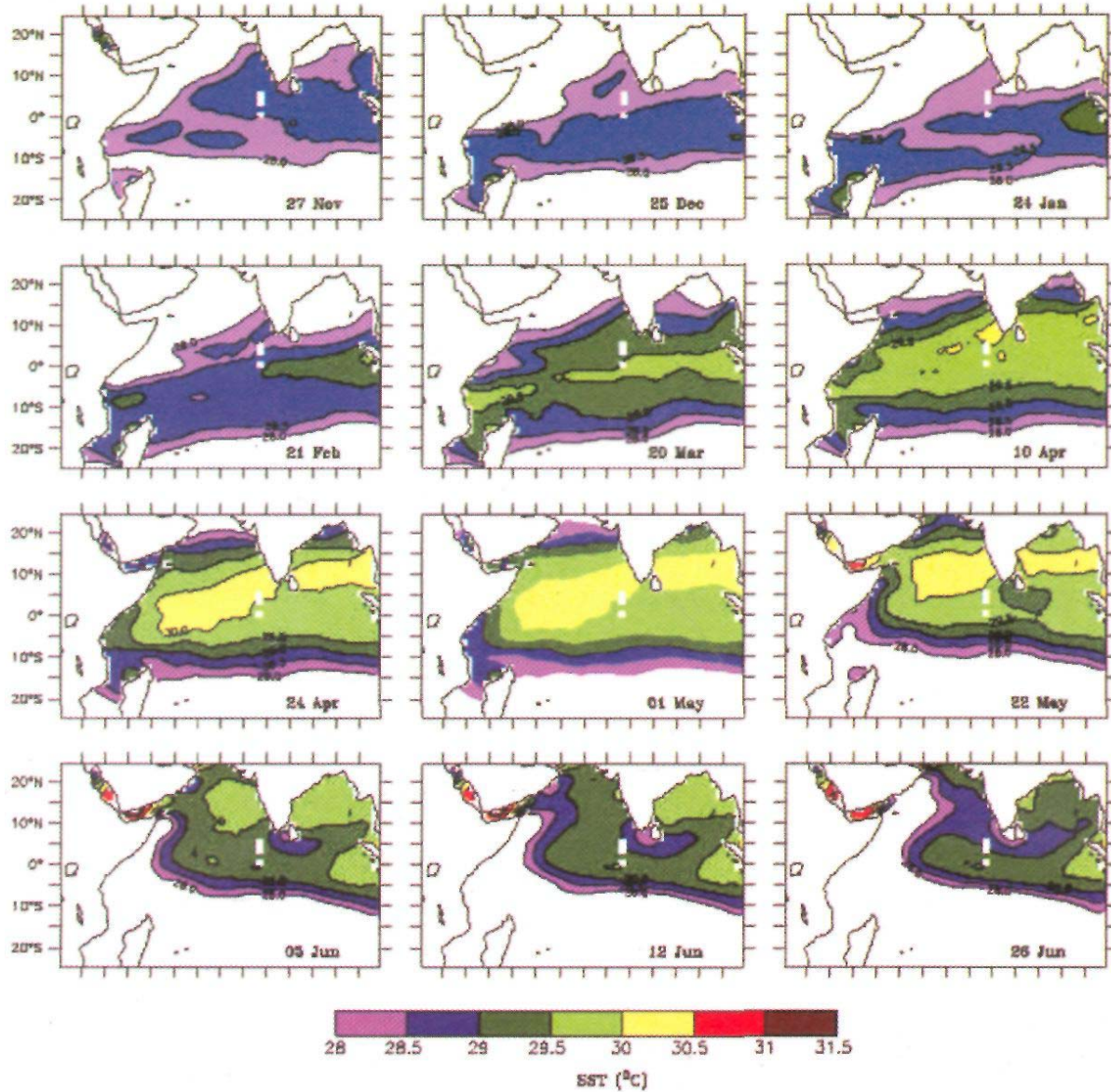


Fig. 5. Evolution of climatological weekly SST ( $^{\circ}\text{C}$ ) during November-June. SSTH in the Lakshadweep Sea is still seen though not as sharp as in Fig. 3 because of averaging done over 14 years

( $\text{SST} < 28^{\circ}\text{C}$ ). Note that the SEAS warms as well as cools earlier than the region to its west; the cooling of the SEAS is not related to the cooling off Somalia.

The pattern of SST evolution is not very different for other years too, though the inter-annual variability is considerable (Fig. 4). Fig. 5 shows the evolution of SST in the climatology based on 14 years of data (1982-95). The SSTH in the Lakshadweep Sea is still visible, but it is not as conspicuous as in Fig. 3 because of averaging. The amplitude and phase of seasonal cycle of SST also suggest that the SSTH precedes the warming of the surroundings

due to the northward movement of the band of warm SST (Fig. 1 in Sheno *et al.*, 1999).

The sea level anomalies (SLA) obtained from the TOPEX/Poseidon satellite altimeter shows high sea level in the SEAS during November (Fig. 6). In December, sea level rises further indicating the formation of the LH in the SEAS. In the week centered 25 December 2002, it spreads over a larger area and moves westward. In January the core of high sea level moves farther west (10-day cycle centered 15 and 29 January 2003). In February, that core moves westward leaving a series of eddies in the

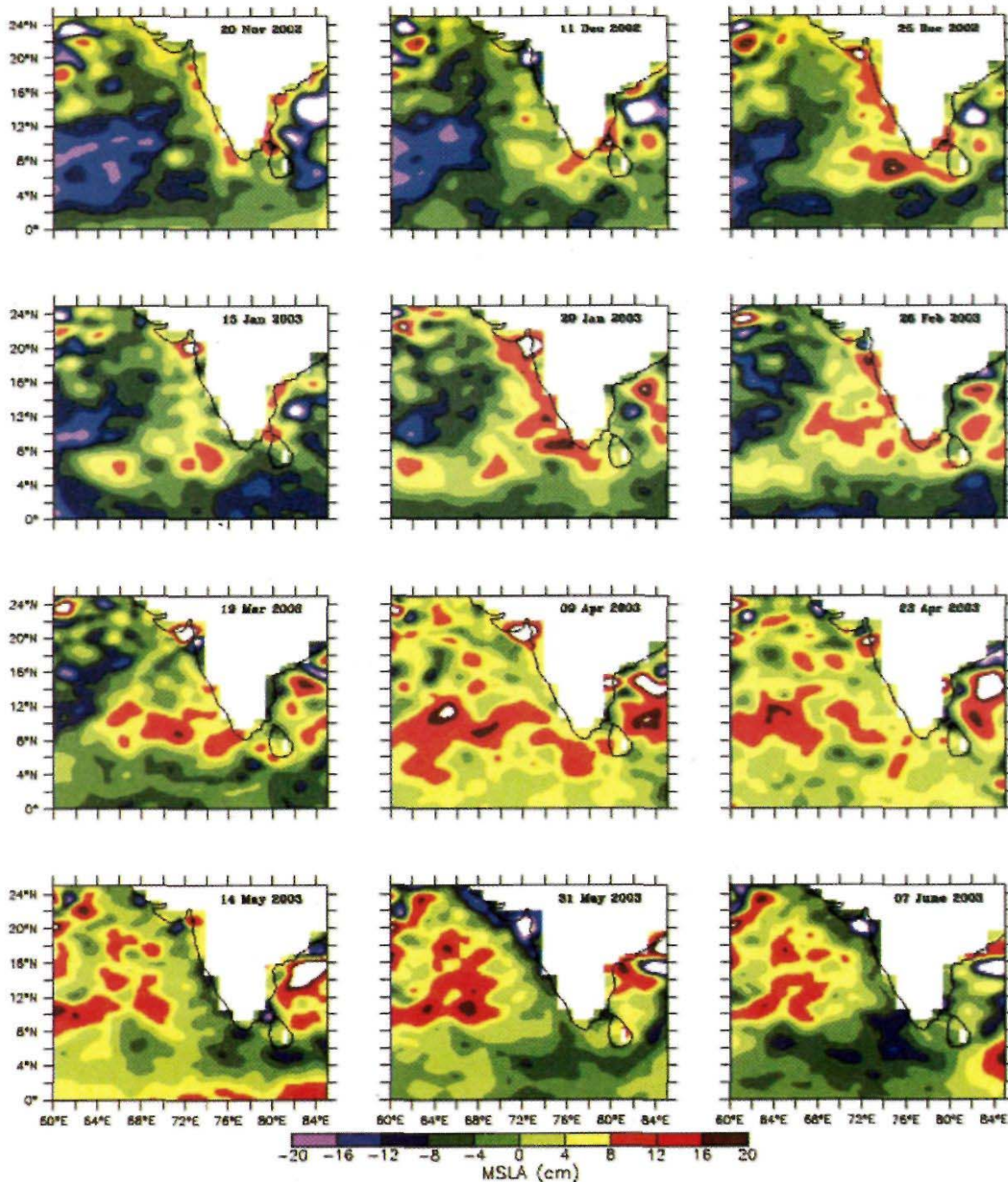


Fig. 6. Evolution of sea level anomaly (SLA, cm) in the SEAS during November 2002 - June 2003. The anomalies in the Lakshadweep Sea are positive during November-April and negative during May-June. The red patches, reflecting high sea level, first form near the coast off southwest India, before they move away towards west. These positive (negative) anomalies in sea level were called Lakshadweep high (Lakshadweep Low) by Shankar and Shetye (1997)

region. In May, sea level is low in the SEAS; the core of low sea level also propagates westward (10-day cycle centered on 14 and 31 May). In early June (7 June), sea level falls below 12 cm. In summary, the SLA is positive

in the SEAS during November-April and negative during May-October; both (high and low SLA) propagate westward. Shankar and Shetye (1997) identified the high and low SLA as a manifestation of the annual cycle of sea

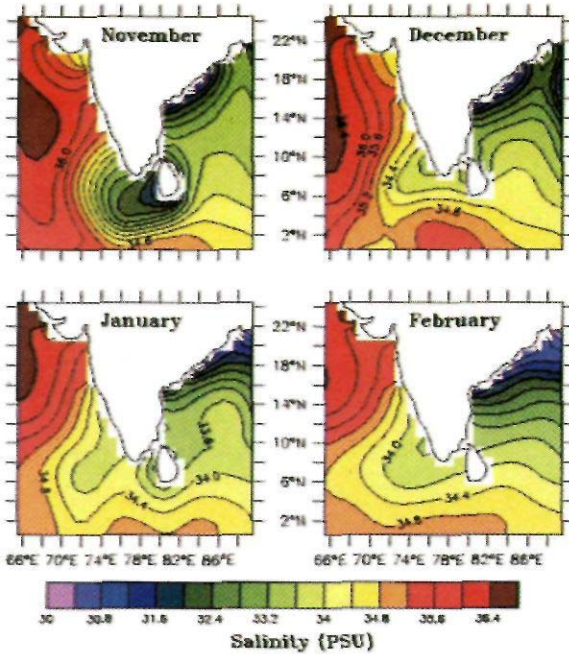


Fig. 7. Evolution of climatic surface salinity (PSU, Levitus *et al.*, 1994) in the north Indian Ocean. Low-salinity water (33.5 PSU) from the Bay of Bengal enters the SEAS in November

level in the SEAS (the low in sea level was called Lakshadweep Low), and associated them with the annual cycle of Kelvin and Rossby waves in the NIO.

The evolution of SST and SSH in the SEAS and the surroundings imply the following. (i) The Lakshadweep Sea begins to warm much before the rest of the SEAS, (ii) the warming in the Lakshadweep Sea is not related to the movement of the band of warm SST that closely follows the movement of the Sun, (iii) a high in sea level in the Lakshadweep Sea (LH) precedes the formation of the SSTH, (iv) both the LH as well as the SSTH first appear on the eastern side of the Lakshadweep Sea and then spread towards south-southwest, and (v) SST collapses below  $28^{\circ}\text{C}$  in the SEAS before it does so in the region to its west and this cooling is independent of that off Somalia.

### 3. Evolution of salinity in the SEAS

The currents along the coast of India are seasonal and they reverse direction (Shetye *et al.*, 1990, 1991a & b, 1993 and 1996). Off the west coast of India the West India Coastal Current (WICC) flows northward during the winter (November-February) and southward during summer (May-September) monsoons. Along the east coast

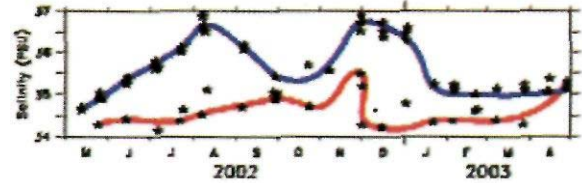


Fig. 8. Evolution of surface salinity (PSU) observed for eastern (red line) and western (blue line) circles in Fig. 2(b). Note that the salinity drops sharply in end-November in the eastern circle and in end-December in the western circle

the EICC flows southward in winter and transports low-salinity water down south. The EICC joins the Winter Monsoon Current (WMC) that flows westward south of Sri Lanka and ultimately feeds the WICC flowing towards north (McCreary *et al.*, 1993, Shankar, 2000; Han and McCreary, 2001, Schott and McCreary, 2001, Shankar *et al.*, 2002; also see the schematic in Fig. 1). The transportation of low-salinity water from the Bay of Bengal into the SEAS in November-December is evident in the climatology of Levitus *et al.* (1994) (Fig. 7).

The surface salinity measurements during the XBT surveys in the Lakshadweep Sea (May 2002 - April 2003) support this contention (Fig. 8); the surface salinity drops suddenly by  $\sim 1$  PSU in end-November 2002 corresponding to the influx of Bay of Bengal water, and it continues to remain low through February before increasing slowly in March. The drop in salinity first occurs in the east and later in the west (end-December), indicating that the low-salinity water first appears in the east and then spreads westward. In February 2003, surface salinity everywhere in the Lakshadweep Sea was below 35 PSU. The numerical simulations of Durand *et al.* (2004) reproduced the westward spread of low-salinity water and attributed it to the westward shift of the current associated with the Rossby waves radiated from the west coast of India.

The arrival of low-salinity water in the SEAS enhances the stratification and hence the stability of the water column. Though no measurement of the stability of the water column was made in November-December, the measurements in March-April and May-June 2003 indicated higher stability for the water column in March-April than in May-June.

### 4. Temperature inversions in the SEAS

An immediate consequence of the enhanced stratification due to the influx of low-salinity water is the formation of a barrier layer (BL), a layer between the

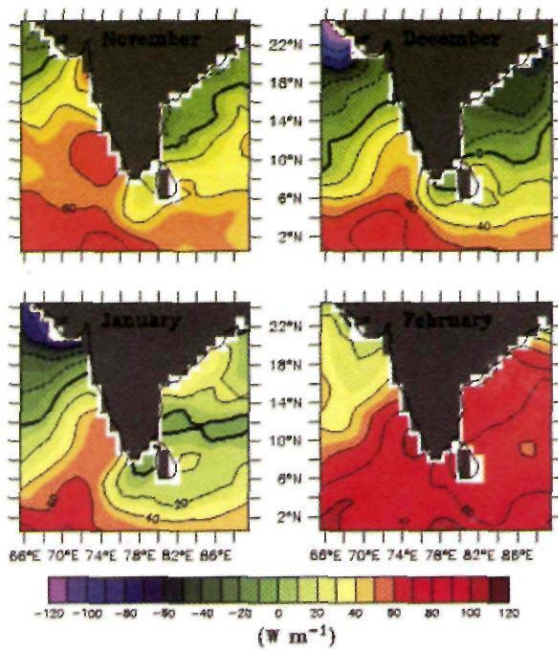


**Fig. 9.** Net surface flux (sum of shortwave radiation, long wave radiation and sensible and latent heat fluxes,  $\text{Wm}^{-2}$ ) over the Arabian Sea and Bay of Bengal during November-February based on the climatology of Josey *et al.*, (1996). Note that the net flux over Bay of Bengal and southern tip of India is negative, which indicates heat lost from the ocean

mixed layer and the thermocline. A BL is formed because the isothermal layer (IL) (say, the layer in which temperature is not more than  $1^\circ\text{C}$  less than SST) is thicker than the mixed layer (ML) (say, the layer in which density does not exceed that at the surface by a specified amount). In such a situation, the incoming shortwave radiation is not absorbed entirely within the ML; some part of it penetrates below the ML, resulting in the IL being thicker than the ML, giving rise to a BL (Vialard and Delecluse, 1998). The BL is called so because it acts as a barrier to entrainment cooling of the surface ML. Climatological data from SEAS (Sprintall and Tomczak, 1992; Rao and Sivakumar, 2003) and the data from ARGO profiling floats (Ravichandran *et al.*, 2004) have shown the existence of a BL below the low-salinity surface mixed layer during winter. XBT data from the SEAS have also shown the presence of inversions in the temperature profile (Thadathil and Gosh, 1992). These inversions occur in the BL, one reason for their existence being the penetration of solar heat flux below the ML.

Transportation of cool low-salinity water over a warmer saline region also can generate inversions. The low-salinity water that was brought into the SEAS from

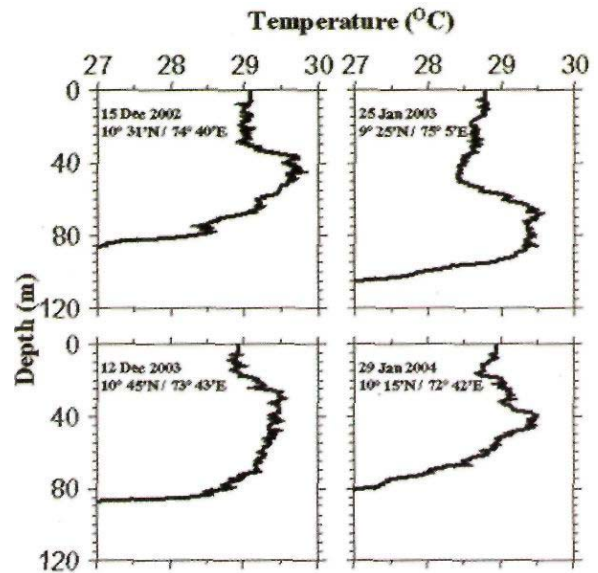


**Fig. 10.** Temperature profiles obtained using XBTs from the Lakshadweep Sea in winter. Note that the subsurface inversions are of the order of  $0.5^\circ\text{C}$

the Bay of Bengal is cooled at the surface en-route to the Lakshadweep Sea owing to net heat flux out of the ocean. The cooling of surface waters occurs at two locations, first in the southern Bay of Bengal during November-December owing to a sharp decrease in the net shortwave radiation (Hastenrath and Lamb, 1979) and again off the southern tip of India (Hastenrath and Lamb, 1979; Luis and Kawamura, 2000), where the latent heat flux increases sharply in January (Fig. 9). The BL thermodynamic effect, together with the cooler low-salinity surface water from the Bay of Bengal, leads to the formation of inversions in the SEAS (Shankar *et al.*, 2004). This was an important observation that emerged from the XBT surveys. The XBT observations made during May 2002 to May 2003 (Shankar *et al.*, 2004) clearly showed the formation of inversions in December 2002 (Fig. 10). By early February 2003, 85% of the XBT profiles in the Lakshadweep Sea showed strong inversions, up from just 10% in November-December 2002. During the XBT survey of 15-19 November 2003, they had already formed and spread towards southwest. Similarly, they appeared all over the Lakshadweep Sea in December 2003 itself, when the SST started increasing due to increased solar insolation. They were observed till end-February and disappeared in March 2004 (Fig. 11). The differences in the formation and spread of inversions during 2002-03 and 2003-04 show that interannual variability is considerable in the amount of freshwater in the SEAS and the timing of its arrival in the region. This was a new finding during ARMEX-II:

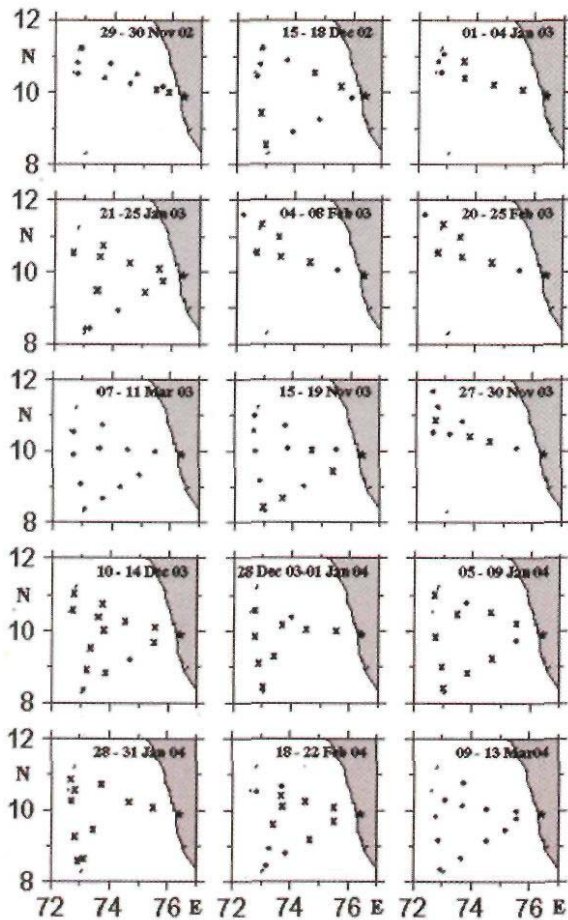


**Fig. 11.** Spatial and temporal distribution of temperature inversions in the Lakshadweep Sea observed using XBTs. The dots indicate the locations of temperature profiles with no inversions and the crosses indicate the locations of profiles with inversions. Note that the inversions first formed in the east in November 2002 before they spread all over in February 2003. Inversions disappeared in March. The pattern is similar during November 2003 to March 2004, though some differences in timing of formations are noticeable

though temperature inversions in the SEAS during winter were also reported earlier (Thadathil and Gosh, 1992), their importance and spread were not known till more XBT data became available from this region under the aegis of ARMEXII.

Shankar *et al.*, (2004) showed that the inversions first formed on the eastern side of the Lakshadweep Sea, then spread towards west, and filled the entire region by February 2002 (Figs. 11 & 12). The westward propagation is clearly shown in the model simulations of Durand *et al.*, (2004) and Shankar *et al.*, (2004) (Fig. 12). The estimated

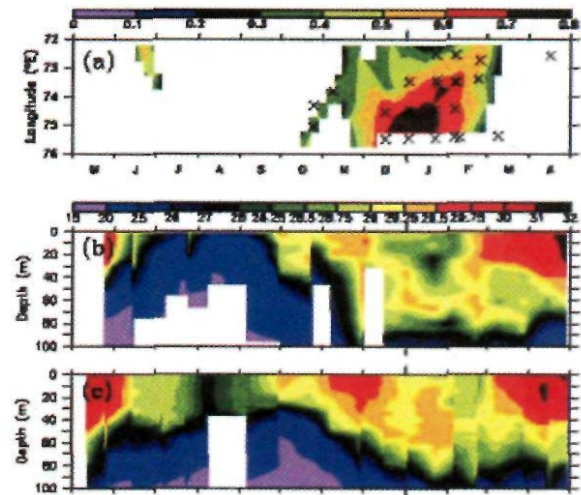


**Fig. 12(a-c).** Evolution of temperature inversions in the Lakshadweep Sea (after Shankar *et al.*, 2004). (a) Time-longitude plot of temperature inversion ( $^{\circ}\text{C}$ ) along  $10.44^{\circ}\text{N}$  from climatological model simulation of Durand *et al.*, (2004). The colour gives the magnitude of temperature inversion; absence of colour indicates absence of inversion. The crosses superimposed on the model field mark the locations where temperature inversions occur in the XBT data along the best-sampled track between Kochi and northwestern Lakshadweep Sea; the model section bisects this track [Fig. 2(b)], (b) Time-depth plot of XBT temperature, smoothed with a 5-point running mean, for eastern circle in the Lakshadweep Sea [Fig. 2(b)], (c) as in (b) but for western circle

speed of propagation of inversions is  $10\text{ cm s}^{-1}$  at  $10^{\circ}\text{N}$  (Shankar *et al.*, 2004), which is comparable to the speed of annual Rossby waves estimated from altimeter and hydrographic observations close to this area (Brandt *et al.*, 2002). In the model, the Rossby wave appears as a second baroclinic mode. Capturing this westward spread of salinity and temperature inversions in data was possible because of the fortnightly sampling of the SEAS under the XBT programme.

## 5. Impact of temperature inversions on SST

The numerical simulations of Durand *et al.*, (2004) showed that the temperature inversions contribute to increasing SST in the initial stages of the formation of the SSSH. Durand *et al.*, (2004) used the OPA OGCM (Madec *et al.*, 1998), which has a horizontal resolution of  $0.5^{\circ}$  and a vertical resolution of 10 m in the upper 120 m. It resolves a state-of-the-art vertical physics based on a

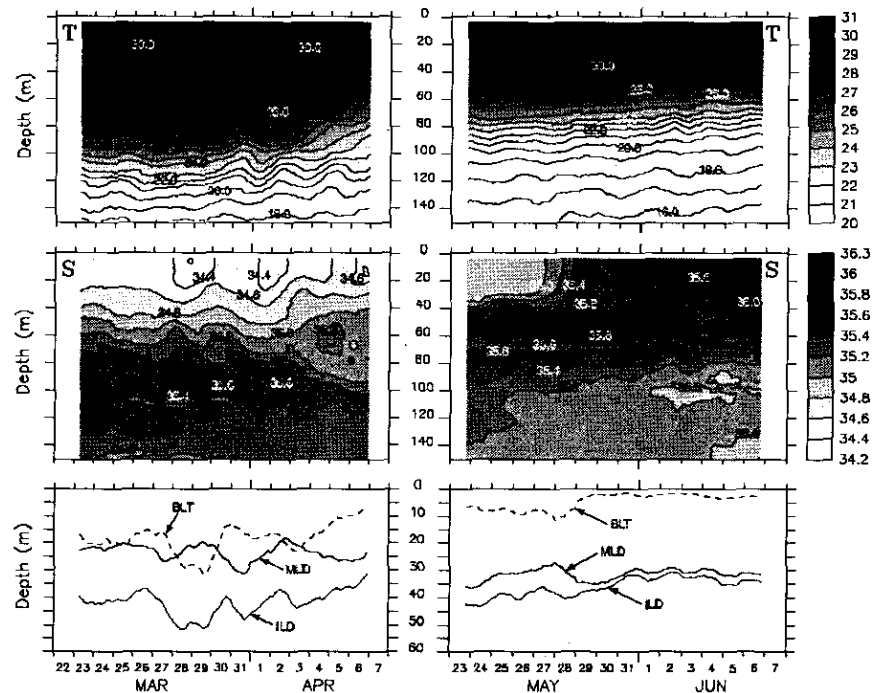


Fig. 13. Time series during 22 March - 7 April (left) and 23 May - 7 June 2003 (right) at  $74^{\circ} 30' \text{ E}$ ,  $9^{\circ} 13' \text{ N}$  in the SEAS of temperature ( $^{\circ}\text{C}$ , top), salinity (PSU, middle), and isothermal-layer depth (ILD), mixed-layer depth (MLD), and barrier layer thickness (BLT) (bottom). The measurements were made every two hours and have been filtered with a 25-hour running mean. This Fig. has been reproduced from Shenoi *et al.*, (2004).

prognostic equation for turbulent kinetic energy (Blanke and Delecluse, 1993). The atmospheric boundary conditions include surface fluxes of momentum, heat, and freshwater. Extensive validation of the simulation revealed that it could successfully reproduce the observed patterns of monsoon circulation as well as basin-scale thermohaline structure of the NIO (Durand *et al.*, 2004). The simulated SST matched very well with the weekly SST of Reynolds and Smith (1994) (Fig. 1 in Durand *et al.*, 2004), and the simulated salinity field matched well with the surface salinity observed along IX-10 XBT line that cuts across the SEAS.

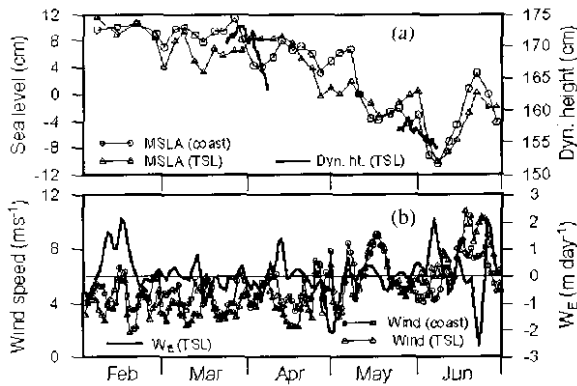
The heat budget of the SEAS estimated from the model simulations showed that during November-March, the ML gains heat from the BL below it; inversions exist in this BL, making it an 'inversion layer'. The integrated effect (during December-February) of the heating of the ML by the inversion layer was  $1.1^{\circ} \text{ C}$ , while the contribution from the surface forcing was  $-0.3^{\circ} \text{ C}$  (Durand *et al.*, 2004); the negative sign indicates cooling.

Shenoi *et al.*, (1999) had hypothesised a connection between the dynamics and thermodynamics of the SEAS.

Shankar *et al.*, (2004) and Durand *et al.*, (2004) showed that the hypothesis was correct. Shenoi *et al.*, (1999) had suggested that down welling and a low-salinity cap ensured that entrainment cooling of the surface was not possible. According to them, therefore, the ocean did nothing to decrease SST, thereby playing a passive role in the evolution of the SSTH. The numerical results of Durand *et al.*, (2004), however, suggest that the ocean plays instead an active role in the formation of the SSTH, with the presence of inversions, which are a consequence of ocean dynamics and thermodynamics, contributing significantly to heating the surface. This is one of the key results of the oceanic component of ARMEX-II.

## 6. Evolution of the barrier layer in the SEAS

Shenoi *et al.*, (2004) described the evolution of the BL in the SEAS using time-series measurements of temperature-salinity profiles obtained every two hours using a CTD; the time-series location (TSL) was in the core of the SSTH [Fig. 2(a)]. The time-series measurements (Fig. 13) during the two cruises in March-April and May-June 2003 clearly showed the evolution of the BL, which was responsible for the formation of



Figs. 14(a&b). Satellite-based observations during February-June 2003. (a) Altimeter sea level anomaly (SLA, cm) at the coast and at lime series location ( $74^{\circ} 30' E$ ,  $9^{\circ} 13' N$ ) in the SEAS, and dynamic height (cm) computed from the time series data, (b) QuikScat winds ( $\text{ms}^{-1}$ ) at the coast and al the ARMEX-II TSL. and the Ekman pumping velocity ( $\text{m day}^{-1}$ ) at TSL. This Fig. has been reproduced from Sheno *et al.*, (2004)

inversions during winter. With the increase in solar insolation in March, the inversions had disappeared by the time of the March-April time series. The BL, however, survived till late May. The BL is thicker during March-April (20 m on an average) than during May-June ( $< 5$  m) (Fig. 13, bottom panel). The depth of the IL (ILD) showed a decreasing trend during March-April owing to upwelling, which is evident in the temperature profiles. However, no such trend is evident in the depth of the ML (MLD). Both ILD and MLD showed some deepening and shallowing corresponding to bursts of low-salinity water on a couple of occasions, resulting in thickening and thinning of the BL.

The most important inference that emerges from Fig. 13 is that the thickness of the BL (BLT) gradually reduced in response to the upwelling, and that the changes in the MLD played a minor role in thinning the BL. The BL collapsed from a thickness of 23 m early on 3 April to 7 m late on 6 April in response to the spurt in upwelling. Based on the corresponding changes in ILD and MLD, Sheno *et al.*, (2004) estimated that 75% of the decrease in BLT came from the decrease of ILD. The correlations between the rates of change of BLT and ILD are much higher (0.741, significant at 99.99%) than between the rates of change of MLD and BLT (0.432, significant at 95%), confirming that the BLT is affected primarily by changes in ILD during March-April.

During May-June, there were changes in three factors compared to March-April. (i) The winds strengthened [Fig. 14(b)], (ii) solar radiation increased,

and (iii) surface salinity increased (Fig. 13, middle panel). Responding to these changes, the MLD also thickened during May-June. Upwelling continued during May-June and so did the decreasing trend in ILD. On 28 May, the MLD increased rapidly owing to an influx of high-salinity water and the BLT collapsed below 5 m on 29 May. Thereafter the BL never recovered owing to the continued presence of high-salinity water. During this period, the changes in ILD and MLD affected the BLT equally: the correlation between the rates of change of ILD and BLT (MLD and BLT) is 0.426 (0.450), both significant at 95%.

This was the second key result of the ARMEX-II oceanic observations. The ocean, whose dynamics is responsible for upwelling and, through the changes in current direction, for the inflow of high-salinity water, plays an active role in the annihilation of the BL, in whose genesis too it played an active role.

## 7. What caused the upwelling?

It is clear that upwelling caused the thinning of the BL. Later, the influx of high-salinity water speeded up the process of annihilation of the BL. Two questions now arise. (i) What caused the upwelling, local winds or remote forcing, and (ii) what caused the advection of high salinity water into the SEAS in late May?

The upwelling seen in the temperature structure during March-April and May-June appears to have started much earlier in February. The altimeter SLA shows a gradual fall since February [Fig. 14(a)]. The altimeter data compare well (in general) with the dynamic heights computed from the time series of temperature-salinity profiles (though the upwelling burst in early April is much weaker in the altimeter data). On an average, the winds measured by QuikScat near the coast as well as at the TSL (which is about 200 km offshore) were weak ( $\sim 4 \text{ ms}^{-1}$ ) [Fig. 14(b)] during March-April. They strengthened slightly (average  $\sim 6 \text{ ms}^{-1}$ ) during May-June. These satellite measurements are in good agreement with the winds measured on board using automatic weather stations. The winds do not show appreciable change before the upwelling burst during 3-7 April. The Ekman pumping velocities computed from the winds are shown in Fig. 14(b); the time integrals of Ekman pumping velocities during 23 March to 7 April show that it forces down welling (sinking;  $-3$  m) rather than upwelling. On the contrary, the  $25^{\circ} \text{C}$  isotherm shows an upliftment of 25 m (Fig. 13, left upper panel). During 23-28 May also, Ekman pumping does not force upwelling; it forces down welling, but the magnitude is negligible ( $\sim 0.2$  m). This implies that the upwelling observed at the TSL during March-April, as well as till 28 May, was not forced

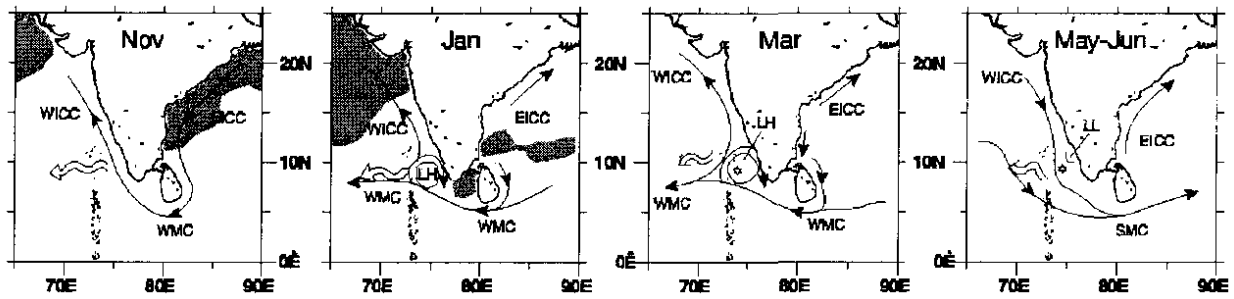


Fig. 15. Schematic showing the evolution of circulation in the SEAS during November-June. The acronyms are as follows: EICC, East India Coastal Current; WMC, Winter Monsoon Current; WICC, West India Coastal Current; LH, Lakshadweep (sea level) high and LL, Lakshadweep (sea level) low. In November, the EICC feeds into the westward WMC south of India. The westward radiation of Rossby waves, depicted by the wiggly arrow, leads to the formation of the LH by January. The WICC flows equatorward off the southwest coast of India, forcing upwelling in a narrow band hugging the coast, but it flows poleward along rest of the west coast. By March, the LH, now slightly displaced offshore, spreads farther westward and the SSTH forms over the LH. In May, the WICC reverses its direction all along the west coast of India and flow equatorward bringing high-salinity water from the northern Arabian Sea. The upwelling that appeared near the coast in January spreads farther west and results in the formation of the LL. The LL and the influx of high salinity water from the north hasten the annihilation of barrier layer leading to the collapse of the SSTH and MWP early in June. The shaded regions show the areas of net surface flux loss by the ocean

by local winds in the SEAS, either through the local generation of coastal Kelvin waves, or through Ekman pumping. After 28 May, the Ekman pumping velocities are positive and lift the isotherm by 7 m; the observed upliftment of the isotherm is 15 m. This implies that after 28 May, the local winds were also important in forcing upwelling, but were ineffective before that. If the upwelling before 28 May is not forced locally, then the only possible cause is remote forcing.

Numerical simulations have shown that the LH and the associated early upwelling off southwest India are forced remotely by the winds that blow along the east coast of India (McCreary *et al.*, 1993; Shankar and Shetye, 1997; Shankar *et al.*, 2002). Local forcing of upwelling starts much later in May (Shankar *et al.*, 2002, their Figs. 19 and 20); during 2003, local forcing of upwelling starts after 28 May. Along the Indian west coast, salinity increases northward at the surface (Shenoi *et al.*, 1993). The poleward-flowing WICC in winter (Shetye *et al.*, 1991a) reverses direction in summer (Shetye *et al.*, 1990). Remote forcing drives the equatorward WICC during May (Shankar *et al.*, 2002); this brings high-salinity water from the north into the SEAS. Hence, both processes that contribute to the annihilation of the BL in the SEAS, upwelling as well as the influx of high salinity water into the SEAS, are forced remotely.

## 8. Summary and discussion

ARMEX-II was designed to test the hypothesis that the ocean plays a major role in the evolution of the SSTH in the Lakshadweep Sea, and to investigate the role of the

SSTH and the MWP, in which the SSTH is embedded, in the formation of the monsoon onset vortex over the SEAS. Shenoi *et al.* (1999) had hypothesised that the downwelling associated with the LH and the cap of low-salinity water ensure that the ocean prevents entrainment cooling, the ocean thereby playing a passive role in the formation of the SSTH. Rao and Sivakumar (1999) had also concluded that the near-surface stratification provided by the low-salinity water is important for the formation of the MWP in the SEAS. In March-April, the radiative heat input overwhelms the turbulent heat loss at the air-sea interface, leading to the formation of the MWP.

The XBT observations show temperature inversions occurring in the Lakshadweep Sea on the arrival of low-salinity water from the Bay of Bengal in November 2002. The inversions are seen initially in the eastern Lakshadweep Sea, but gradually spread westward along with the low-salinity water. By February, inversions are observed all over the Lakshadweep Sea, with 85% of the XBT profiles showing a temperature inversion, up from just 10% in November. Model simulations also show the existence and westward spread of temperature inversions in conjunction with the low-salinity water and the LH, providing the required link between ocean dynamics and thermodynamics. The inversions exist in a BL, which is one of the two possible causes of the inversions. The second cause is cooling due to a decrease in shortwave radiation in the southern Bay of Bengal during November-January and an increase in latent heat flux near the southern tip of India during January. The inversions heat the mixed layer above, implying an active role for the ocean in the formation of the SSTH unlike the passive role hypothesised earlier.

The inversions disappear by March, when SST increases owing to the increase in solar insolation, but the CTD observations on board ORV Sagar Kanya show that the BL continues to exist till late May, when it is finally annihilated. The CTD time-series observations in the Lakshadweep Sea, in conjunction with satellite data and numerical simulations, show that the thinning of the BL is initiated by remotely forced upwelling during March-April. Upwelling persists in thinning the BL even in May, but its final annihilation is due to the advection of high-salinity water from the north by an equatorward WICC, this reversal in current also being forced remotely. The annihilation of the BL paves the way for the subsequent collapse of the SSTH and the MWP. Thus, the ocean also plays an active role in the annihilation of the SSTH.

This sequence of events is summarised in the schematic in Fig. 15. Thus, the ARMEX-II observations show that oceanic processes play an active role in both the genesis and annihilation of the SSTH and the MWP in the SEAS. In addition, remote forcing of ocean dynamics in the region is a key player in the thermodynamics of the SEAS.

Thus, as described in this paper, the oceanic component of ARMEX-II has been successful in fulfilling the first of two ARMEX-II objectives, investigating the role of oceanic processes in the life cycle of the SSTH in the Lakshadweep Sea. The second objective, to investigate the possible connection between the SSTH or MWP and the monsoon onset vortex, calls for an integration of the results of the oceanic and atmospheric components of ARMEX-II and for focused modelling studies.

#### Acknowledgements

The altimeter SLA, Quikscat winds, and weekly SST data were downloaded from the web sites of AVISO, SSMI, and R.W. Reynolds, respectively. G.S. Bhat provided the wind data from ORV Sagar Kanya. We thank DST and DOD for financial support, including ship time. We thank our colleagues who participated in Sagar Kanya and XBT cruises for data collection, and the masters and crew of ORV Sagar Kanya, MV Tipu Sultan and MV Bharat Seema for their assistance during the cruises. Ms. Pramila Gawas, R. Uchil and A. Mahale helped with most of the Figs. Fabien Durand was funded by the Indo-French centre for Environment and Climate. The software packages FERRET and UTC were used extensively. This is NIO contribution 3940.

#### References

Blanke, B. and Delecluse, P., 1993, "Variability of the tropical Atlantic Ocean simulated by a general circulation model with two different mixed layer physics", *J. Phys. Oceanogr.*, 23, 1363-1388.

- Brandt, P., Stramma, L., Schott, F., Fischer, J., Dengler, M. and Quadfasel, D., 2002, "Annual Rossby waves in the Arabian Sea from TOPEX/Poseidon altimeter and *in situ* data". *Deep-Sea Res.* 11,49, 1197-1210.
- Bruce, J. G., Johnson, D. R. and Kindle, J. C., 1994, "Evidence for eddy formation in the eastern Arabian Sea during the northeast monsoon", *J. Geophys. Res.*, 99, 7651-7664.
- Bruce, J. G., Kindle, J. C., Kantha, L. H., Kerling, J. L. and Bailey, J. E., 1998, "Recent observations and modeling in the Arabian Sea Laccadive High region", *J. Geophys. Res.*, 103, 7593-7600.
- Durand, F., Shetye, S. R., Vialard, J., Shankar, D., Sheno, S. S. C., Ethe, C. and Madec, G., 2004, "Impact of temperature inversions on SST evolution in the southeastern Arabian Sea during the pre-summer monsoon season", *Geophys. Res. Lett.*, 31, L01305, doi: 10.1029/2003GL018906.
- Gadgil, S., Srinivasan, J., Nanjundiah, R. S., Krishnakumar, K., Munoi, A. A. and Rupakumar, K., 2002, "On forecasting the Indian summer monsoon : The intriguing summer of 2002", *Curr. Sci.*, 83, 394-403.
- Han, W. and McCreary, J. P., 2001, "Modeling salinity distributions in the Indian Ocean", *J. Geophys. Res.*, 106, 859-877.
- Hastenrath, S. and Lamb, P., 1979, "Climatic atlas of the Indian Ocean", Pan II : Heat budget. Tech. Rep.. University of Wisconsin. Madison.
- Joseph, P. V., 1990, "Warm Pool over the Indian Ocean and Monsoon Onset", *Tropical Ocean-Atmos. News Lett.*, 53, 1-5.
- Josey, S. A., Kent, E. C., Oakley, D. and Taylor, P. K., 1996, "A new global air sea heat and momentum flux climatology". *International WOCE News Letter*, 24, 3-5.
- Krishnamurti, T. N., Ramanathan, P. A. Y. and Pasch, R., 1981, "On the on-set vortex of the summer monsoon", *Mon. Wea. Rev.*, 109, 344-363.
- Levitus, S., Burgett, R. and Boyer, T. P., 1994, "World Ocean Atlas 1994", Vol. 3. Salinity, NOAA Atlas NESDIS 3, 99. U.S. Govt. Print. Off., Washington, D.C.
- Luis, A. J. and Kawamura, H., 2000, "Wintertime wind forcing and sea surface cooling near the south India tip observed using NSCAT and AVHRR", *Rem. Sens. Environ.*, 73, 55-64.
- Madec, G., Delecluse, P., Imbard, M. and Levy, C., 1998, "OPA 8.1 Ocean General Circulation Model reference manual". Note du Pole de modelisation, Institut Pierre-Simon Laplace (IPSL), France, °N 11, p91.
- McCreary, J. P., Kundu, P. K. and Molinari, R. L., 1993, "A numerical investigation of the dynamics, thermodynamics and mixed-layer processes in the Indian Ocean", *Prog. Oceanogr.*, 31, 181-244.
- McCreary, J. P., Han, W., Shankar, D. and Shetye, S. R., 1996, "Dynamics of the East India Coastal Current, 2. Numerical solutions", *J. Geophys. Res.*, 101, 13,993-14,010.

- Rao, R. K. and Sivakumar, R., 1999, "On the possible mechanisms of the evolution of a mini-warm pool during the pre-summer monsoon season and the onset vortex in the southeastern Arabian Sea", *Q. J. R. Meteorol. Soc.*, 125, 787-809.
- Rao, R. R. and Sivakumar, R., 2003. "Seasonal variability of sea surface salinity and salt budget of the mixed layer of the north Indian Ocean", *J. Geophys. Res.*, 108, 3009. doi:10.1029/2001JC000907.
- Ravichandran, M., Vinayachandra, P. N., Joseph, S. and Radhakrishnan, K., 2004, "Results from the first Argo float deployed by India", *Curr. Sci.*, 86, 651-659.
- Reynolds, R. and Smith, T., 1994, "Improved global sea surface temperature analyses using optimum interpolation". *J. Climate*, 7, 929-948.
- Schott, F. and McCreary, J. P., 2001. "The monsoon circulation in the Indian Ocean", *Progr. Oceanogr.*, 51, 1-123.
- Sengupta, D., Ray, P. K. and Bhat, G. S., 2002, "Spring warming of the eastern Arabian Sea and Bay of Bengal from buoy data", *Geophys. Res. Lett.*, 29, doi: 10.1029/2002GL015340.
- Shankar, D., McCreary, J. P., Han, W. and Shetye, S. R., 1996, "Dynamics of the east India coastal current. 1, Analytic solutions forced by interior Ekman pumping and local alongshore winds", *J. Geophys. Res.*, 101, 13,975-13,991.
- Shankar, P. and Shetye, S. R., 1997, "On the dynamics of the Lakshadweep high and low in the southeastern Arabian Sea", *J. Geophys. Res.*, 102, 12,551-12,562.
- Shankar, D., 2000. "Seasonal cycle of sea level and currents along the coast of India", *Curr. Sci.*, 78, 279-288.
- Shankar, D., Vinayachandran, P. N. and Unnikrishnan, A. S., 2002, "The monsoon currents in the north Indian Ocean", *Progr. Oceanogr.*, 52, 63-120.
- Shankar, D., Gopalakrishna, V. V., Shenoi, S. S. C., Durand, F., Shetye, S. R., Rajan, C. K., Zacharias, J., Araligidad, N. and Michael, G. S., 2004, "Observational evidence for westward propagation of temperature inversions in the southeastern Arabian Sea", *Geophys. Res. Lett.*, 31. doi:10.1029/2004GL019652.
- Shenoi, S. S. C., Shetye, S. R., Gouveia A. P. and Micheal, G. S., 1993, "Salinity extrema in the Arabian Sea, Monsoon Biogeochemistry. Edited by V. Ittikot and R. R. Nair, Im Selbstverlag des Geologisch-Palaontologischem Instituts des Universitat Hamburg. 37-50.
- Shenoi, S. S. C., Shankar, D. and Shetye, S. R., 1999, "On the sea surface temperature high in the Lakshadweep Sea before the onset of the southwest monsoon", *J. Geophys. Res.*, 104(C7), 15,703-15,712.
- Shenoi, S. S. C., Shankar, D. and Shetye, S. R., 2002. "Differences in heat budgets of the near-surface Arabian Sea and Bay of Bengal: Implications for the summer monsoon", *J. Geophys. Res.*, 107, doi 10.1029/2000JC000679.
- Shenoi, S. S. C., Shankar, D. and Shetye, S. R., 2004, "Remote forcing annihilates barrier layer in southeastern Arabian Sea", *Geophys. Res. Lett.*, L05307, doi:10.1029/2003GL019270.
- Shetye, S. R., Gouveia, A. D., Shenoi, S. S. C., Sundar, D., Michael, G. S., Almeida, A. M. and Santanam, K., 1990, "Hydrography and circulation off the west coast of India during southwest monsoon", *J. Mar. Res.*, 48, 359-378.
- Shetye, S. R., Gouveia, A. D., Shenoi, S. S. C., Michael, G. S., Sundar, D., Almeida, A. M. and Santanam, K., 1991a, "The coastal current off western India during the northeast monsoon", *Deep-Sea Res.*, 38, 1517-1529.
- Shetye, S. R., Shenoi, S. S. C., Gouveia, A. D., Michael, G. S., Sundar, D. and Nampoothiri, G., 1991b. "Wind-driven coastal upwelling along the western boundary of Bay of Bengal during southwest monsoon", *Cont. Shelf Res.*, 11, 1397-1408.
- Shetye, S. R., Gouveia, A. D., Shenoi, S. S. C., Sundar, D., Michael, G. S. and Nampoothiri, G., 1993. "The western boundary current of the seasonal subtropical gyre in the Bay of Bengal", *J. Geophys. Res.*, 98, 945-954.
- Shetye, S. R., Gouveia, A. D., Shankar, D., Shenoi, S. S. C., Vinayachandran, P. N., Sundar, D., Michael, G. S. and Nampoothiri, G., 1996, "Hydrography and circulation in the western Bay of Bengal during the northeast monsoon". *J. Geophys. Res.*, 101, 14,011-14,025.
- Sprintall, J. and Tomczak, M., 1992, "Evidence of the barrier layer in the surface layer of the tropics", *J. Geophys. Res.*, 97, 7305-7316.
- Thadathil, P. and Gosh, A. K., 1992. "Surface Layer Temperature Inversion in the Arabian Sea during Winter", *J. Oceanogr.*, 48, 293-304.
- Vialard, J. and Delecluse, P., 1998, "An OGCM study for the TOGA decade. Part II : Barrier layer formation and variability", *J. Phys. Oceanogr.*, 28, 1089-1106.
- Vinayachandran, P. N. and Shetye, S. R., 1991, "The warm pool in the Indian Ocean", *Proc. Ind. Acad. Sci. (Earth Planet. Sci.)*, 100, 165-175.
- Vinayachandran, P. N., Shetye, S. R., Sengupta, P. and Gadgil, S., 1996. "Forcing mechanisms of the Bay of Bengal circulation". *Curr. Sci.*, 71, 753-763.